hNaa10p contributes to tumorigenesis by facilitating DNMT1-mediated tumor suppressor gene silencing

Chung-Fan Lee,[1,2,3] Derick S.-C. Ou,[2,4] Sung-Bau Lee,[2] Liang-Hao Chang,[2] Ruo-Kai Lin,[2] Ying-Shiuan Li,[2] Anup K. Upadhyay,[5] Xiaodong Cheng,[5] Yi-Ching Wang,[6] Han-Shui Hsu,[7] Michael Hsiao,[2] Cheng-Wen Wu,[1,3,8,9] and Li-Jung Juan[1,2]

[1]Institute of Molecular Medicine, College of Medicine, National Taiwan University, Taipei, Taiwan. [2]Genomics Research Center, Academia Sinica, Taipei, Taiwan. [3]Institute of Cancer Research, National Health Research Institutes, Zhunan, Taiwan. [4]Institute of Molecular and Cellular Biology, National Tsing Hua University, Hsinchu, Taiwan. [5]Department of Biochemistry, Emory University School of Medicine, Atlanta, Georgia, USA. [6]Department of Pharmacology, College of Medicine, National Cheng Kung University, Tainan, Taiwan. [7]Division of Thoracic Surgery, Department of Surgery, Taipei Veterans General Hospital, National Yang-Ming University School of Medicine, Taipei, Taiwan. [8]Institute of Biomedical Sciences, Academia Sinica, Taipei, Taiwan. [9]Institute of Biochemistry and Molecular Biology, National Yang-Ming University, Taipei, Taiwan.

Hypermethylation-mediated tumor suppressor gene silencing plays a crucial role in tumorigenesis. Understanding its underlying mechanism is essential for cancer treatment. Previous studies on human N-α-acetyltransferase 10, NatA catalytic subunit (hNaa10p; also known as human arrest-defective 1 [hARD1]), have generated conflicting results with regard to its role in tumorigenesis. Here we provide multiple lines of evidence indicating that it is oncogenic. We have shown that hNaa10p overexpression correlated with poor survival of human lung cancer patients. In vitro, enforced expression of hNaa10p was sufficient to cause cellular transformation, and siRNA-mediated depletion of hNaa10p impaired cancer cell proliferation in colony assays and xenograft studies. The oncogenic potential of hNaa10p depended on its interaction with DNA methyltransferase 1 (DNMT1). Mechanistically, hNaa10p positively regulated DNMT1 enzymatic activity by facilitating its binding to DNA in vitro and its recruitment to promoters of tumor suppressor genes, such as E-cadherin, in vivo. Consistent with this, interaction between hNaa10p and DNMT1 was required for E-cadherin silencing through promoter CpG methylation, and E-cadherin repression contributed to the oncogenic effects of hNaa10p. Together, our data not only establish hNaa10p as an oncoprotein, but also reveal that it contributes to oncogenesis through modulation of DNMT1 function.

Introduction

Aberrant DNA methylation is one of the major characteristics of cancer development. Many cancer cells have been observed with higher DNA methyltransferase (DNMT) activity (1–4), which is believed to contribute to the CpG island hypermethylation of tumor suppressor genes (5). DNA methyltransferase 1 (DNMT1), the major DNMT in adult cells, catalyzes DNA methylation by transferring the methyl group from the donor S-adenosyl methionine (AdoSAM) to the fifth carbon of cytosine (6, 7). How its activity is regulated in cancer cells is an important issue. It has been shown that the methyltransferase activity of DNMT1 can be modulated in several different ways, including (a) regulation of DNMT1 gene expression by Ras (8), Rb (9), and AUF1 (10); (b) regulation of DNMT1 protein stability by DNMT1 methylation and demethylation mediated by SET7 (11) and LSD1 (11, 12), respectively; and (c) protein-protein interaction with G9a (13), EZH2 (14), and PML-RAR (15).

The highly conserved arrest-defective 1 (ARD1) protein family, recently named N-α-acetyltransferase 10, NatA catalytic subunit (Naa10p, encoded by *NAA10*; ref. 16), was originally described as an N-α-acetylase for the first amino acid of specific subsets of nascent polypeptides (17, 18). The yeast Naa10p has previously been shown to control mating type switch (19), protein stability (20), gene silencing (21, 22) and cell cycle progression (19). Mouse Naa10p–mediated (mNaa10p-mediated) acetylation at the oxygen-dependent degradation domain (ODD) of HIF1α promotes HIF1α degradation (23). This property inversely links Naa10p to cancer, as HIF1α upregulation is essential for vascular angiogenesis required for cell invasion (23, 24). However, the role of human Naa10p–mediated (hNaa10p-mediated) HIF1α regulation in cancer has been controversial (25–27). hNaa10p is also reported to prevent tumor cell migration and cell invasion by acetylating and inactivating the myosin light chain kinase required in cell motility (28) and to repress tumorigenesis by decreasing cell proliferation and inducing autophagy (29). In contrast to the tumor suppressor function, hNaa10p has been shown to possess a role in cell proliferation (27, 30), anti-G_1 arrest (30), and apoptosis (31, 32) and to promote the function of the oncoprotein β-catenin (30). The oncogenic potential of hNaa10p is further supported by its increased protein level in tumor tissues (33–35). How hNaa10p contributes to tumorigenesis is unclear (36, 37). In the current study, we identified that hNaa10p acts as an oncoprotein that represses the expression of tumor suppressor genes by facilitating DNMT1 function.

Results

To determine whether hNaa10p functions as an oncoprotein or a tumor suppressor, we first analyzed its mRNA and protein levels in human lung cancer tissues by quantitative real-time RT-PCR and immunohistochemistry (IHC), respectively. Consistent with

Authorship note: Derick S.-C. Ou and Sung-Bau Lee contributed equally to this work.

Conflict of interest: The authors have declared that no conflict of interest exists.

Citation for this article: *J Clin Invest.* 2010;120(8):2920–2930. doi:10.1172/JCI42275.

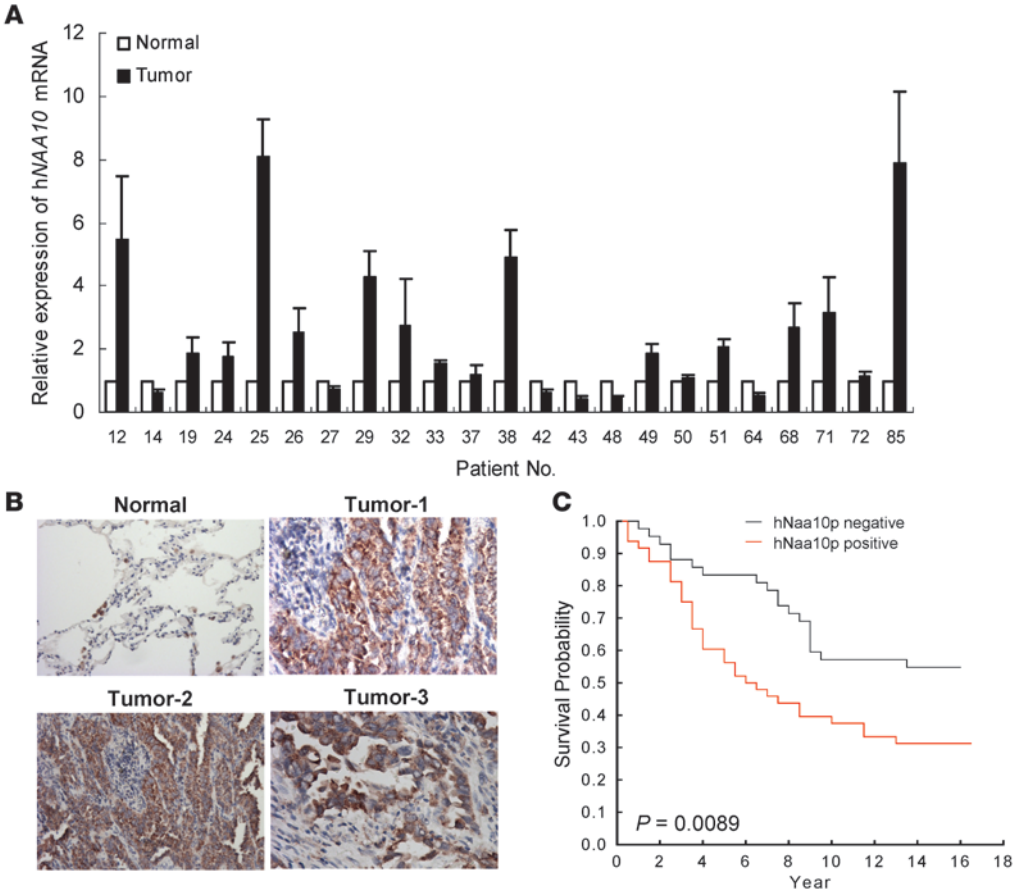

Figure 1

hNaa10p overexpression in human lung cancer tissues. (**A**) Relative mRNA level of h*NAA10* in lung cancerous specimens or surrounding non-neoplastic stroma tissues after normalization to actin. Data are mean ± SD from 3 independent assays. (**B**) IHC detection of hNaa10p protein in normal and cancerous human lung tissues. Shown are 1 example of normal adjacent tissue and 3 examples of tumor sections. Original magnification, ×100 (left panels); ×200 (right panels). (**C**) IHC analysis of 90 lung adenocarcinoma patients indicated that 48 patients with high hNaa10p protein level in tumor tissues showed poor survival compared with 42 patients with hNaa10p expression below the detection limit, as in normal adjacent tissues. $P = 0.0089$.

previous reports (33, 34), cancerous specimens had increased levels of hNaa10p protein and mRNA compared with their surrounding non-neoplastic stroma tissues (Figure 1, A and B). In 23 sample pairs, 4 (17%) had equal h*NAA10* mRNA levels, 6 (26%) showed decreased levels of h*NAA10* mRNA in cancer tissues, and 13 (57%) exhibited higher levels of h*NAA10* mRNA in cancer tissues (Figure 1A). Importantly, the 48 lung cancer patients found to have higher levels of hNaa10p had poor prognosis and/or survival compared with the 42 patients with hNaa10p expression levels that were below the detection limit, as in normal adjacent tissues ($P = 0.0089$; Figure 1C). These results indicate that hNaa10p was overexpressed in more than half of human lung cancer tissues examined, and the survival analysis further suggests hNaa10p may play a role in lung cancer progression.

In agreement with this correlative study, enforced expression of hNaa10p in NIH3T3 cells increased its colony formation capacity (Figure 2A), which indicates that hNaa10p promotes anchorage-independent growth, a characteristic of cell transformation. Next, we sought to determine whether hNaa10p is necessary for the proliferation of lung cancer cells. We introduced 2 independent siRNAs against h*NAA10* (referred to herein as h*NAA10*-1 and h*NAA10*-2) to H1299 lung cancer cells, which express high levels of hNaa10p, and analyzed the effect of hNaa10p knockdown on cell proliferation ability. Figure 2B shows the efficient depletion of the endogenous hNaa10p by these 2 siRNAs, but not by scrambled siRNA (si-scramble) or siRNA against HTLV Tax protein (si-Tax; ref. 38). Consistent with previous reports (27, 30), knockdown of hNaa10p reduced lung tumor cell proliferation (Figure 2C). Furthermore, hNaa10p loss of function, achieved by transient introduction of siRNAs into cells (Figure 2D), or stable depletion of hNaa10p by lentivirus infection of shRNAs (Supplemental Figure 1; supplemental material available online with this article; doi:10.1172/JCI42275DS1), greatly reduced the colony formation potential. To substantiate these in vitro observations, we analyzed whether suppression of hNaa10p impairs the ability of lung cancer cells to form tumors in mice. H1299 cells with controls (mock and si-scramble) or siRNA against h*NAA10* were subcutaneously injected into NOD-SCID mice. Knockdown of hNaa10p greatly impaired the tumorigenesis potential of the human lung cancer cells in mice (Figure 2E).

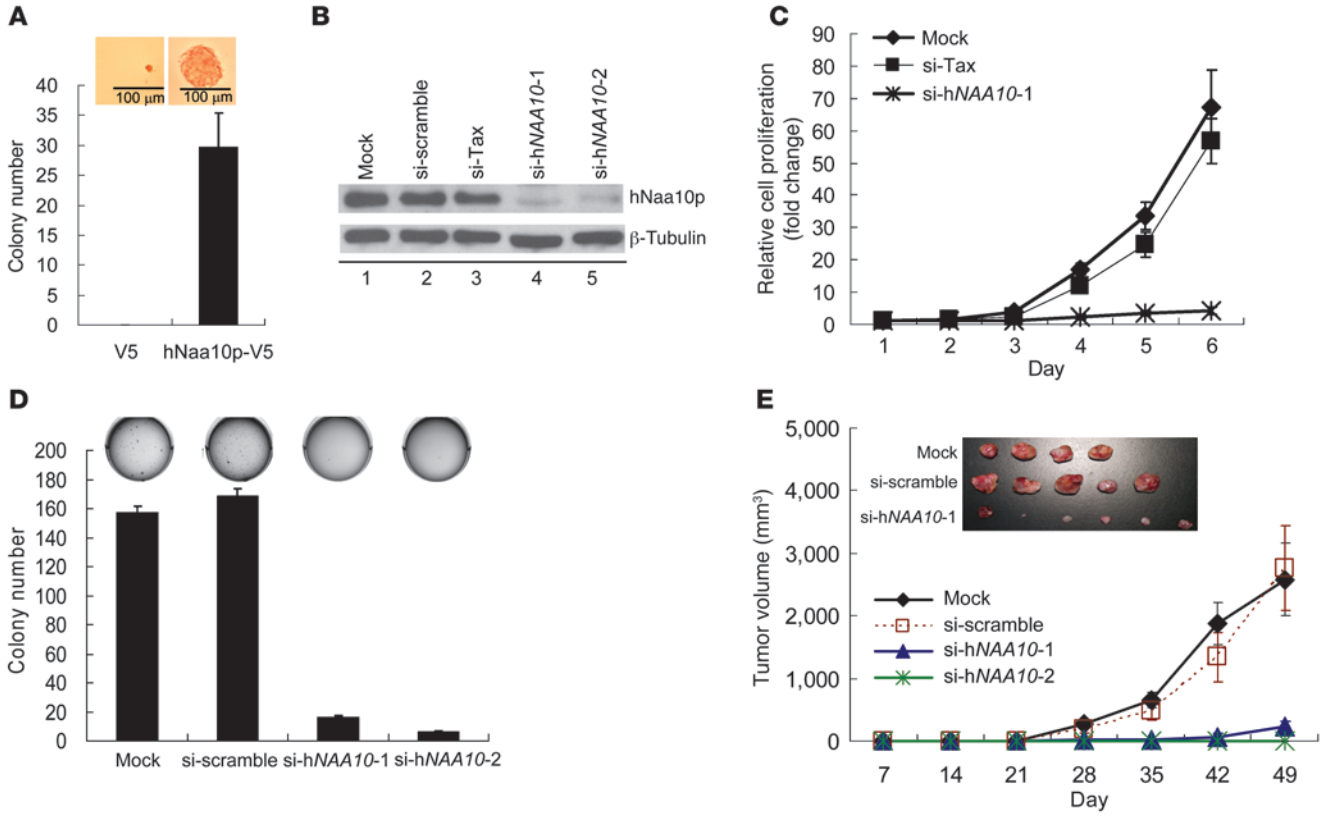

Figure 2

hNaa10p contributes to clonogenesis and xenograft tumor formation in lung cancer cells. (**A**) hNaa10p overexpression enhances the colony formation ability of NIH3T3 cells on soft agar. hNaa10p-V5, hNaa10p with C-terminal V5 tag (containing 14 amino acids, GKPIPNPLLGLDST, derived from the P and V proteins of the paramyxovirus of simian virus 5). Representative microscopic images of the colonies are shown. Scale bars: 100 μm. (**B**) Western blots showing successful knockdown of hNaa10p protein level by si-h*NAA10*-1 and si-h*NAA10*-2. si-scramble and si-Tax were used as negative controls. (**C**) Lung cancer H1299 cells transfected with si-h*NAA10*-1 exhibited poor proliferation rate compared with cells mock transfected or transfected with si-Tax. (**D**) Transfection with si-h*NAA10*-1 or si-h*NAA10*-2 impaired the ability of H1299 cells to form colonies on soft agar, compared with cells mock transfected or transfected with si-scramble. Photographs of representative soft agar plates are shown. (**E**) H1299 cells transfected with si-*hNAA10*-1 or si-h*NAA10*-2 generated smaller tumors in NOD-SCID mice than did cells mock transfected or transfected with si-scramble. The volume of the derived tumors was measured at the indicated days after injection. Representative tumor masses are shown. A total of 5–6 mice was analyzed in each group. Data in **A**, **C**, **D**, and **E** are mean ± SD from 3 independent assays.

The levels of hNaa10p in the excised tumor masses at the end point are shown in Supplemental Figure 2. Collectively, our in vitro and in vivo observations support that hNaa10p functions as an oncoprotein.

To understand the mechanism by which hNaa10p contributes to oncogenesis, we attempted to identify hNaa10p functional partners. A yeast 2-hybrid screen using hNaa10p as bait identified DNMT1 as an hNaa10p-interacting protein (data not shown). The interaction of the 2 proteins was verified in H1299 cells by co-IP assay (Figure 3A and Supplemental Figure 3). Interestingly, the hNaa10p Ab specifically precipitated DNMT1, but not DNMT3a or DNMT3b (Figure 3A). Deletion studies identified aa 291–570 of DNMT1 as being important for hNaa10p association (Figure 3B). Consistently, only the purified GST-fused DNMT1 containing aa 291–570 precipitated the in vitro translated hNaa10p (Figure 3C) and His-Xpress–tagged hNaa10p expressed in and purified from *E. coli* (Figure 3D), which indicates that the domain alone is sufficient to bind to hNaa10p and the interaction of hNaa10p and DNMT1 is direct. Conversely, a 21-aa fragment of hNaa10p (aa 102–122) appeared to be necessary and sufficient to mediate hNaa10p interaction with DNMT1 (Figure 3E). The equal expression of all GST-DNMT1 derivatives is shown in Supplemental Figure 4.

After defining the interaction domains of hNaa10p and DNMT1, we next analyzed whether the oncogenic potential of hNaa10p depends on its interaction with DNMT1. To this end, the cDNA encoding full-length hNaa10p, or hNaa10p lacking DNMT1 interaction motif (aa 102–122) or an irrelevant region (aa 182–201), was introduced back to H1299 cells depleted of hNaa10p by siRNA. The effect of the deletions on the cell transformation capacity of hNaa10p was analyzed by colony formation assay. Deletion of the DNMT1 interaction motif impaired the ability of hNaa10p to rescue the colony formation capacity of the hNaa10p-depleted cells (Figure 4A, lane 5). In contrast, reexpression of the full-length hNaa10p or a deletion mutant that does not affect its interaction with DNMT1 (aa 182–201) restored the colony formation capability of the hNaa10p-depleted cells (Figure 4A, lanes 3 and 4). The differential effects of these mutants were not the result of their differential expression, as they were expressed at similar levels (Figure 4A, bottom). The DNMT1 interaction domain was important

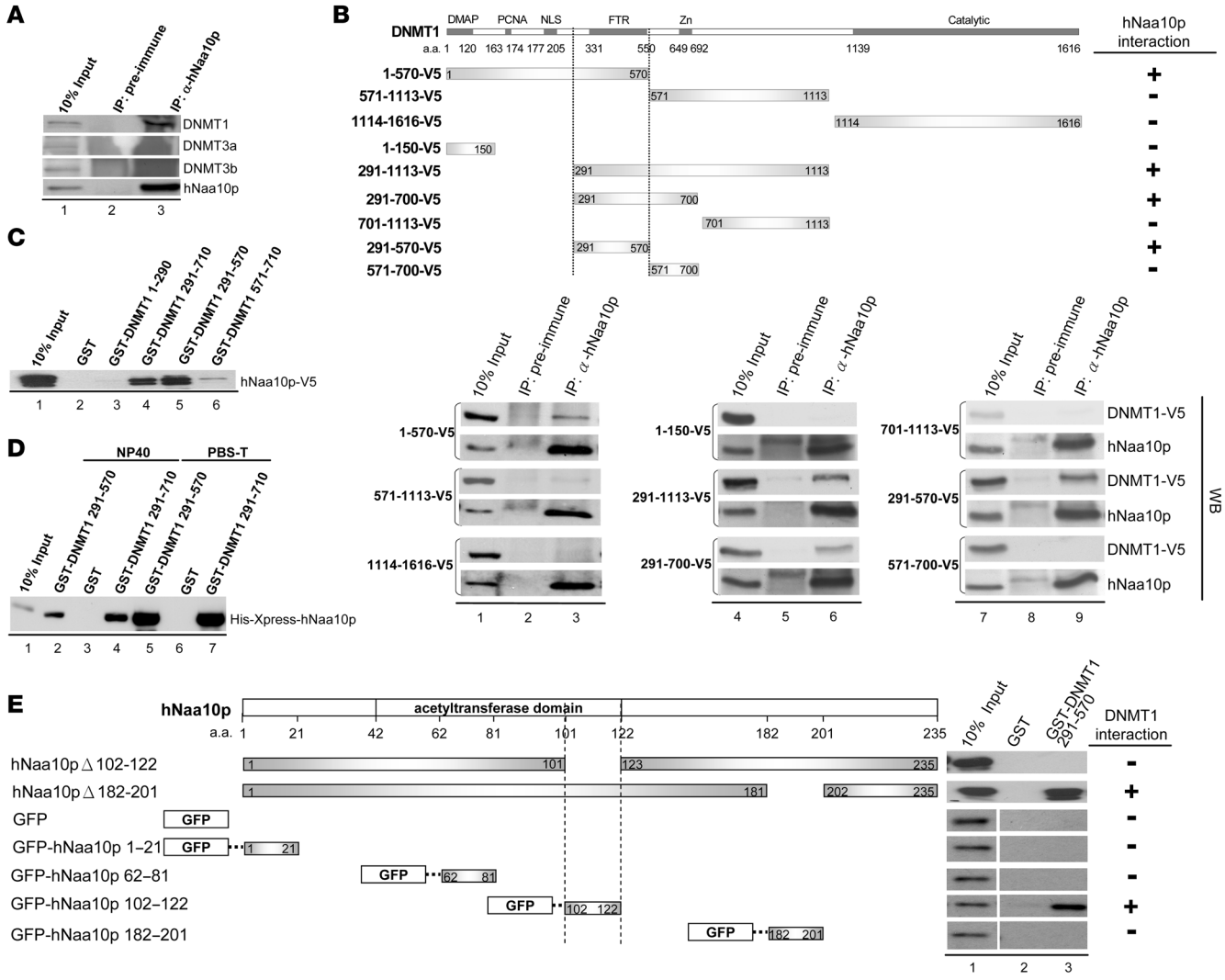

Figure 3

hNaa10p associates with DNMT1 both in vivo and in vitro. (**A**) Co-IP showed that anti-hNaa10p pulled down hNaa10p and DNMT1, but not DNMT3a or DNMT3b, from H1299 cell exacts. (**B**) Co-IP showed that anti-hNaa10p pulled down hNaa10p and all DNMT1 fragments (V5-tagged) containing aa 291–570 exogenously expressed in H1299 cells, as revealed by Western blot using hNaa10p or V5 Ab. The schematic illustration of DNMT1 fragments used here, and the results of interaction, are summarized above. DMAP, DNMT1-associated protein; PCNA, proliferating cell nuclear antigen; NLS, nuclear localization signal; FTR, replication foci targeting sequence. (**C** and **D**) GST pulldown assays showed that the recombinant GST-fused DNMT1 fragments containing aa 291–570 precipitated hNaa10p-V5 in vitro translated from rabbit reticular lysate (**C**) or His-Xpress-hNaa10p expressed in and purified from *E. coli* (**D**), as revealed by Western blot using the respective Abs. In **D**, lanes 2–4 and 5–7 show results using NP40 and PBS-T, respectively, as incubation/wash buffer. (**E**) GST-DNMT1 aa 291–570 was used to pull down the in vitro translated V5-tagged hNaa10p mutant lacking aa 102–122 or aa 182–201, or GFP-fused hNaa10p fragments containing aa 1–21, aa 62–81, aa 102–122, or aa 182–201, followed by Western blotting with V5 or GFP Ab. Lanes were run on the same gel but were noncontiguous (white lines).

for hNaa10p to mediate not only colony formation, but also cell proliferation (Figure 4B). Since deleting the DNMT1 interaction motif (aa 102–122) also eliminated part of the acetyltransferase domain of hNaa10p (Figure 3E), and hNaa10p stimulated the in vivo acetylation of DNMT1 (Supplemental Figure 5), we asked whether hNaa10p-mediated colony formation relies on its acetylase activity. As shown in Supplemental Figure 6A, reintroduction of the siRNA-resistant acetylase-dead mutant hNaa10p R82A (39) still restored colony formation ability, although not to the same degree seen by reexpression of WT hNaa10p. The loss of the acetylase activity of hNaa10p R82A was demonstrated by its failure in autoacetylation compared with WT hNaa10p (Supplemental Figure 6B). Importantly, the mutant still associated with DNMT1 (Supplemental Figure 6C). Together, these data suggest that the oncogenic potential of hNaa10p involves an acetylation-independent mechanism and relies on its interaction with DNMT1.

Hypermethylation of promoter CpG dinucleotides and subsequent inactivation of tumor suppressor genes is believed to contribute to oncogenesis (40–42). Since hNaa10p and DNMT1 interaction is essential for the oncogenic activity of hNaa10p, we analyzed whether hNaa10p can modulate the enzymatic activity of DNMT1. To this end, nuclear lysates from H1299 cells with

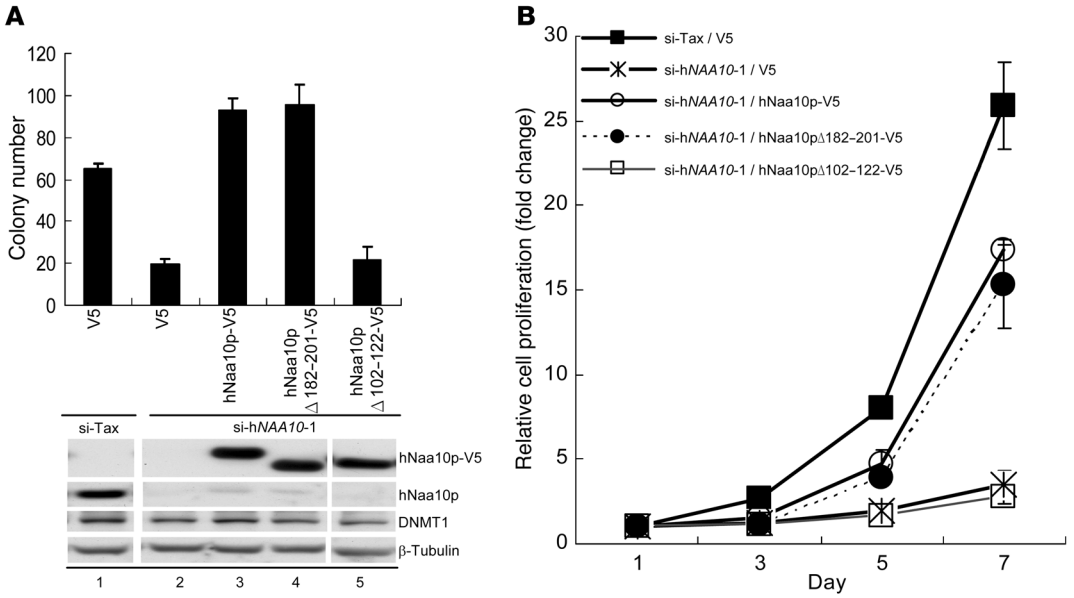

Figure 4

The oncogenic potential of hNaa10p depends on its binding to DNMT1. (**A** and **B**) si-h*NAA10*-1–treated H1299 cells expressing the resistant V5-tagged WT or mutant hNaa10p lacking aa 182–201 or aa 102–122 were subjected to soft agar assay and Western blot (**A**) as well as cell proliferation study (**B**). Data are mean ± SD from 3 independent assays. Lanes in **A** were run on the same gel but were noncontiguous (white lines).

or without the depletion of hNaa10p by siRNA were collected for DNA methylation assay and Western analysis. Knockdown of hNaa10p or DNMT1 greatly reduced the DNMT activity of the nuclear extracts toward poly dI-dC (Figure 5A), which indicates that hNaa10p positively modulates cellular DNMT activity. As controls, we also included nuclear extracts derived from cells transfected with si-Tax or cells treated with 5′-AzadC in parallel assays. Next, we asked whether ectopic expression of hNaa10p increases DNMT activity, and, if so, whether this is linked to the capacity of hNaa10p to acetylate DNMT1 in cells (Supplemental Figure 5). To this end, we expressed WT hNaa10p, hNaa10p R82A, or DNMT1 in cells, followed by DNMT assay and Western analysis. As expected, overexpression of DNMT1 greatly increased DNMT activity (Figure 5B, lane 4). Interestingly, overexpression of both WT and mutant hNaa10p also increased the DNMT activity of the lysates (Figure 5B, lanes 2 and 3), which suggests that the acetylation activity of hNaa10p is not required for hNaa10p to stimulate the enzymatic activity of DNMT1. To further confirm that hNaa10p directly stimulates DNMT1 activity in an acetylation-independent manner, recombinant DNMT1 and hNaa10p were used in a DNMT assay in the absence or presence of acetyl-CoA. The results demonstrated that the capability of hNaa10p to stimulate the enzymatic activity of DNMT1 did not require the presence of acetyl-CoA (Figure 5C, compare lanes 1 and 3). Addition of acetyl-CoA did not further stimulate hNaa10p-mediated upregulation of DNMT1 activity (Figure 5C, compare lanes 3 and 6). Similar results were obtained when differentially methylated DNAs were used as substrates (Supplemental Figure 7). We noted that although hemimethylated DNA was a better substrate for purified DNMT1 (Supplemental Figure 7, compare lanes 1 and 4), hNaa10p increased 7-fold the capacity of DNMT1 to methylate nonmethylated DNA (Supplemental Figure 7, compare lanes 4 and 6).

To understand how hNaa10p stimulates the enzymatic activity of DNMT1, we asked whether hNaa10p facilitates binding of DNMT1 to its substrate by EMSA assays. DNMT1 bound to the biotin-labeled DNA substrate (Figure 5D, lane 2), and, importantly, this binding increased in a hNaa10p dose-dependent manner (Figure 5D, lanes 3–6). Interestingly, hNaa10p alone was able to bind to the hemimethylated DNA probe in a gel with a higher percentage of the polyacrylamide (Supplemental Figure 8, lane 5). Moreover, the hNaa10p-DNA interaction could only be competed by nonmethylated DNA (Supplemental Figure 8, lanes 6–8), but not by fully methylated DNA (Supplemental Figure 8, lanes 9–11). These data collectively allowed us to conclude that hNaa10p stimulates DNMT1 activity by increasing the association of DNMT1 with its substrate DNA and is independent of the acetylase activity of hNaa10p. Next, we analyzed whether hNaa10p facilitates the recruitment of DNMT1 to its targets in cells. We used ChIP assays to analyze DNMT1 binding to the promoter region of the E-cadherin gene (a known DNMT1 target; refs. 38, 43) in H1299 cells with or without overexpression of hNaa10p. Whereas overexpression of hNaa10p greatly increased DNMT1 association with the E-cadherin promoter, this effect was not observed in the p21 promoter (Figure 5E). Importantly, hNaa10p depletion diminished DNMT1 binding, whereas knocking down DNMT1 did not affect hNaa10p association (Figure 5F). Together, these results indicate that hNaa10p facilitates recruitment of DNMT1 to the E-cadherin promoter.

We next investigated whether depletion of hNaa10p affects the level of E-cadherin promoter methylation (Figure 6A). Bisulfite sequencing showed that knockdown of DNMT1 reduced methylation of CpG sites within the E-cadherin promoter from –202 bp to +31 bp (Figure 6B). As expected, the DNA methylation level of the E-cadherin proximal promoter decreased when hNaa10p or DNMT1 was depleted from cells (Figure 6B). Furthermore,

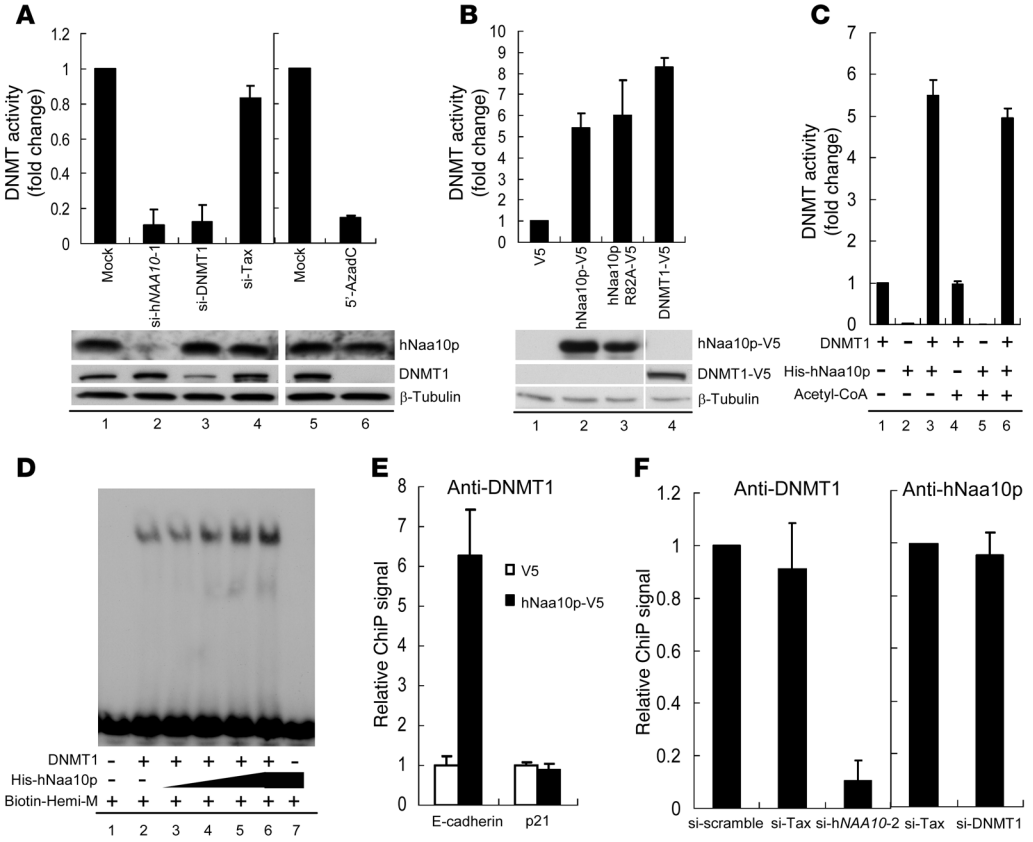

Figure 5

hNaa10p maintains and stimulates DNMT1 activity by increasing DNMT1 binding to DNA. (**A**) H1299 cells transfected with si-h*NAA10*-1 or si-DNMT1 or treated with 5'-AzadC had reduced DNMT activity compared with cells mock transfected or transfected with si-Tax. Western blot shows expression of corresponding proteins. (**B**) Overexpressing WT hNaa10p, acetylase-dead mutant hNaa10p R82A, or DNMT1-V5 increased DNMT activity of 293T cells. (**C**) hNaa10p stimulated DNMT1 activity independently of acetyl-CoA. Recombinantly purified DNMT1 and His-hNaa10p, alone or in combination, were mixed with or without acetyl-CoA, followed by DNMT assay. (**D**) hNaa10p facilitated DNMT1 binding to DNA in vitro. EMSA assays were applied with the biotin-labeled hemimethylated DNA probe alone or with the recombinantly purified DNMT1 in the absence or presence of increasing amounts of *E. coli*–expressed and purified His-hNaa10p. (**E**) ChIP assay showed that enforced expression of vector or hNaa10p in H1299 cells enhanced DNMT1 binding to promoter of E-cadherin, but not p21. (**F**) ChIP showed that depleting hNaa10p from H1299 cells by si-h*NAA10*-2 abolished DNMT1 binding to the E-cadherin promoter, whereas DNMT1 loss of function did not impair hNaa10p binding to the same promoter. Lanes in **A** and **B** were run on the same gel but were noncontiguous (white lines).

overexpression of the siRNA-resistant hNaa10p restored CpG methylation (Figure 6C). It should be noted that methylation of this region has previously been shown to be most tightly associated with loss of E-cadherin expression (43, 44). Thus, consistent with the observation that hNaa10p facilitated the recruitment of DNMT1 to the E-cadherin promoter, hNaa10p also facilitated the corresponding promoter methylation.

To further study whether hNaa10p is indeed involved in the transcriptional regulation of E-cadherin, we tested the reporter activity driven by E-cadherin proximal promoter in the absence or presence of overexpressed hNaa10p. In agreement with the above data, the E-cadherin promoter activity was reduced by hNaa10p in a dose-dependent manner (Supplemental Figure 9A) and increased when hNaa10p was depleted (Supplemental Figure 9B). Importantly, hNaa10p-mediated downregulation of E-cadherin promoter activity was lost when cellular DNMT1 was eliminated (Figure 7A), which indicates that hNaa10p repression of E-cadherin expression depends on DNMT1. Moreover, the hNaa10p mutant lacking DNMT1 interaction domain (aa 102–122) did not repress E-cadherin promoter activity to the same degree as did WT hNaa10p (Figure 7B). Results of the reporter assays were further confirmed by analyzing endogenous E-cadherin expression at the mRNA and protein levels. Depletion of hNaa10p in H1299 cells increased the mRNA and protein levels of E-cadherin (Figure 7, C and D). We noted that siRNA against h*NAA10* frequently increased the DNMT1 protein level (Figure 7D). However, the increased DNMT1 no longer downregulated E-cadherin expression without hNaa10p, consistent with the ChIP results demonstrating that hNaa10p was required for the recruitment of DNMT1 to E-cadherin promoter. Furthermore, reexpression of siRNA-resistant hNaa10p downregulated the protein level of E-cadherin induced by deleting the endogenous hNaa10p (Supplemental Figure 10). Consistently, overexpressing hNaa10p without DNMT1 interaction domain (aa 102–122) failed to cause the same effect (Figure 7E). These results indicate that hNaa10p regulation of E-cadherin expression is not an off-target effect and relies on DNMT1 interaction. Finally, to further confirm that the defective colony formation ability of hNaa10p-depleted cells is

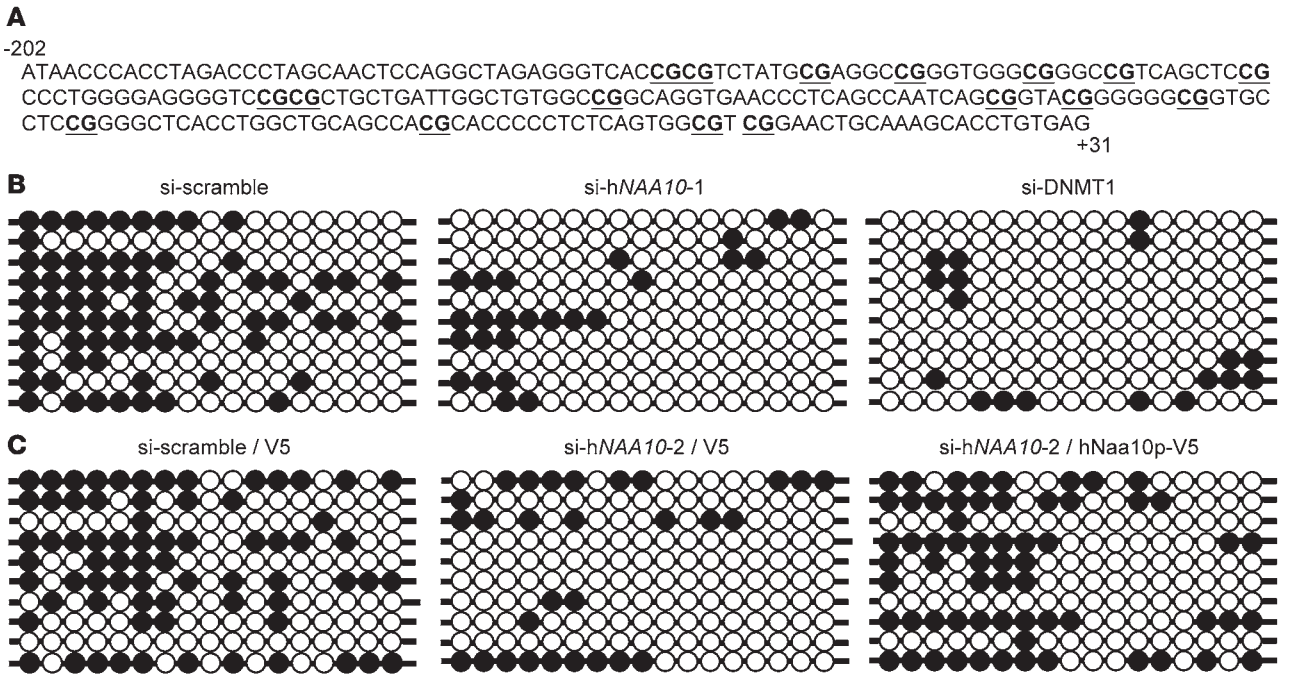

Figure 6

hNaa10p and E-cadherin promoter methylation. (**A**) The sequence of the proximal promoter region –202 to +31 bp of the E-cadherin gene containing 17 CpGs (shown by bold and underline). (**B** and **C**) Bisulfite sequencing analysis. After bisulfite treatment, 10 independent clones of the indicated groups were sequenced. Black circles denote methylated cytosine in specific CpG; white circles denote nonmethylated cytosine in specific CpG. (**B**) Depleting hNaa10p or DNMT1 from H1299 cells reduced E-cadherin promoter methylation. (**C**) Overexpression of siRNA-resistant hNaa10p restored E-cadherin promoter methylation.

caused, at least in part, by reexpression of E-cadherin, we knocked down E-cadherin in hNaa10p-depleted cells; as expected, colony formation ability was partly restored (Figure 7F). Together, our findings suggest that hNaa10p represses E-cadherin expression via recruitment of DNMT1.

Discussion

We have provided in vitro and in vivo evidence demonstrating the oncogenic activity of hNaa10p. We also demonstrated that hNaa10p can interact with DNMT1 and positively regulate DNMT1 enzymatic activity, particularly its de novo DNMT activity for unmethylated DNA (Supplemental Figure 7). Increasing the affinity of DNMT1 to its target DNA, rather than acetylating DNMT1, is likely the mechanism by which hNaa10p modulates DNMT1 activity.

Surprisingly, we found that purified hNaa10p bound to hemimethylated DNA fragments, and the binding could only be disrupted by nonmethylated DNA oligo, not by fully methylated DNA probes (Supplemental Figure 8). Thus, unlike UHRF1, which regulates DNMT1 function by specifically recognizing hemimethylated DNA (45, 46), hNaa10p can interact with both nonmethylated and hemimethylated DNA. Together with the in vivo data showing that (a) hNaa10p was present on the E-cadherin promoter when DNMT1 was depleted (Figure 5F); (b) hNaa10p was required for DNMT1 to associate with the E-cadherin promoter (Figure 5F); and (c) hNaa10p regulated E-cadherin gene expression depending on its interaction with DNMT1 (Figure 7), these observations suggest that hNaa10p likely stabilizes the DNMT1/DNA complex by interacting with both DNMT1 and the target DNA.

Notably, in some cases of cancer, overexpression of DNMT1 does not necessarily result in hypermethylation of its downstream genes (47, 48). Moreover, a number of reports also demonstrate that hypermethylation of some DNMT1 target genes does not require increased DNMT1 expression (49, 50). These observations raise an interesting hypothesis: we believe that regulation of DNMT1 activity and its recruitment to specific DNA plays a more important role than regulation of DNMT1 expression level in fine-tuning the activity of a specific subset of genes. Our present results suggest that hNaa10p can likely bypass the need of DNMT1 overexpression for tumor suppressor gene methylation by increasing the association of existing DNMT1 to its targets.

Whether the acetylase activity of hNaa10p correlates with its function in cancer is not clear. Although β-catenin can be acetylated by hNaa10p, whether acetylation is essential for the oncogenic potential of β-catenin remains unaddressed (30). Tuberous sclerosis 2 (TSC2) was recently shown to be N-α-acetylated by hNaa10p, and the acetylation increases TSC2 protein stability (29). In so doing, hNaa10p represses the mammalian target of rapamycin (mTOR) signaling pathway and thus prevents breast tumorigenesis (29). In the current study, we examined whether acetyltransferase activity is required for hNaa10p to function as an oncoprotein. The colony formation assay (Supplemental Figure 6) and the cell proliferation study (data not shown) both indicated that reexpression of the acetylase-dead hNaa10p R82A mutant still restored the above 2 functions repressed by depleting the endogenous hNaa10p, although not to the same degree as by WT hNaa10p. This observation suggests that an acetylase-independent pathway is involved in hNaa10p-mediated

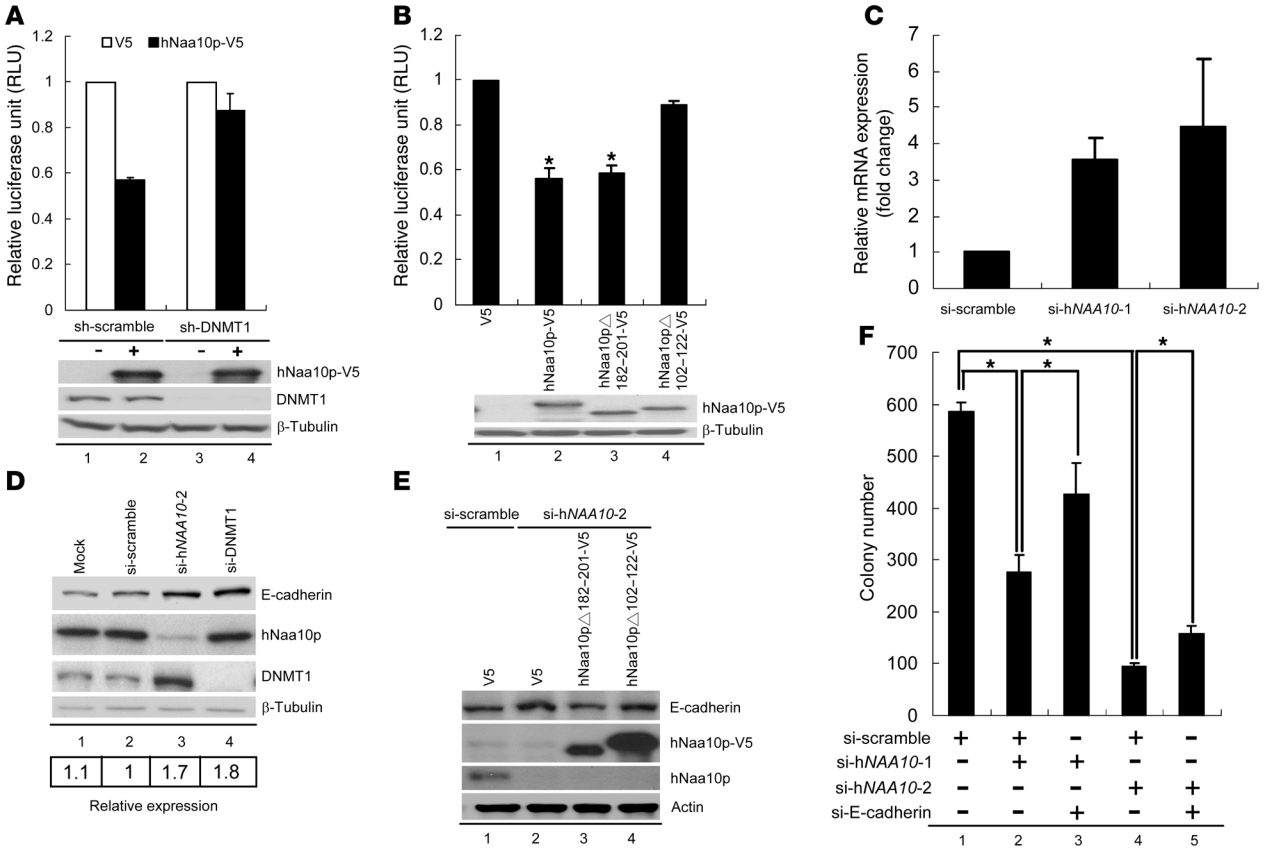

Figure 7

DNMT1-dependent repression of E-cadherin by hNaa10p contributes to hNaa10p oncogenic ability. (**A**) hNaa10p inhibition of E-cadherin promoter activity was dependent on DNMT1. H1299 cells with lentivirus infection of si-scramble or si-DNMT1 were transfected with the luciferase reporter driven by the E-cadherin promoter, together with vector or hNaa10p-V5 expression plasmid, followed by luciferase assay. (**B**) E-cadherin promoter activity was only inhibited by transfected WT hNaa10p or hNaa10p mutant lacking aa 182–201, not by the mutant lacking DNMT1 binding region (aa 102 to 122). (**C** and **D**) Depletion of hNaa10p from H1299 cells increased mRNA (**C**) and protein (**D**) levels of E-cadherin gene. Quantified E-cadherin protein levels (relative to β-tubulin) are shown below the lane numbers. (**E**) Western blot showed that hNaa10p lacking DNMT1 interaction domain (aa 102–122) failed to repress E-cadherin protein level. (**F**) Knocking down E-cadherin partly rescued the colony formation ability inhibited by depleting hNaa10p. The indicated siRNAs were cotransfected into H1299 cells, followed by colony formation assay. All data in **A**, **B**, **C**, and **F** are mean ± SD from 3 independent experiments. *$P < 0.05$.

lung tumorigenesis. Taken together, results from our and others' laboratories suggest that both acetylation-dependent and -independent mechanisms likely contribute to the function of hNaa10p in tumorigenesis in a context-dependent manner.

We provided evidence that hNaa10p plays an important role in the promoter silencing of the tumor suppressor gene E-cadherin, which likely contributes to hNaa10p oncogenic activity. E-cadherin has previously been reported to function in both cell invasion (51) and cell growth (52, 53). Indeed, we showed that knocking down E-cadherin partly restored the colony formation ability inhibited by si-h*NAA10* (Figure 7F), which suggests that E-cadherin and hNaa10p work in the same pathway. In addition to E-cadherin, other genes — including potential tumor suppressors, some of which are known to induce apoptosis (e.g., LATS2 and KLF2; refs. 54–56), and genes known to promote cell cycle arrest — are also upregulated by depleting either hNaa10p or DNMT1 (Supplemental Figure 11). Importantly, by analyzing the expression of these genes available in published microarray databases of lung cancer patients (57–59), we found that expression of E-cadherin, KLF2, QKI-6, and CDKN1C/p57 was inversely correlated with high expression of hNaa10p. LATS2 is a potential tumor suppressor gene downregulated in non–small cell lung carcinoma (NSCLC; ref. 60), and its promoter is hypermethylated in many cancers (61–63). We further demonstrated that depleting hNaa10p reduced DNMT1 binding to the LATS2 promoter (Supplemental Figure 12A) and increased the mRNA (Supplemental Figure 11A) and protein (Supplemental Figure 12B) levels of LATS2, which could only be repressed by reexpression of siRNA-resistant hNaa10p containing DNMT1 interaction domain (Supplemental Figure 12, C and D). In support of this, si-LATS2 partly restored the colony formation repressed by depleting hNaa10p (Supplemental Figure 12E). Thus, in addition to inhibiting E-cadherin expression, repression of LATS2, and other genes mentioned above, may also contribute to the oncogenic function of hNaa10p. It is postulated that regulation of these genes through DNMT1 might be an important mechanism leading to the known phenotypes of hNaa10p in cell proliferation (27, 32), anti-G_1/S arrest (30), and apoptosis (31, 32).

In addition to lung cancer, we also found a negative expression correlation of hNaa10p with KLF2 and QKI-6 in prostate and colon cancers (64, 65), hNaa10p with QKI-6 in bladder cancer (66), and hNaa10p with CDKN1C/p57 in gastric cancer (67). Whether high expression of hNaa10p in these cancers contributes to tumorigenesis remains to be investigated. As mentioned in Introduction, whether hNaa10p is an oncoprotein or a tumor suppressor is still debated (36, 37). In contrast to the oncogenic role of hNaa10p in lung tumorigenesis, we indeed found that depletion of hNaa10p increased the colony formation ability of MCF7, a breast cancer cell line (data not shown). Consistent with our result, hNaa10p was recently reported to inhibit breast cancer formation through mTOR repression (29), as mentioned above. Thus, it seems hNaa10p has distinct role in cells from different cancer types. Whether this involves tissue-specific hNaa10p partners or modifications remains to be investigated.

Methods

Lung cancer patients, clinical sample preparation, real-time PCR assay, and IHC assay. For the h*NAA10* mRNA analysis shown in Figure 1A, tissues were collected after permission from the Institutional Review Board of Veterans General Hospital–Taipei (Taipei, Taiwan) and informed consent from each recruited patient were obtained. Surgically resected tumor samples from 23 patients diagnosed with primary NSCLC admitted to Veterans General Hospital, Taichung and Taipei, were collected between 1993 and 2003. Of these patients, 6 had squamous carcinoma, and 17 had adenocarcinoma. Histological data on tumor types and stages were determined according to World Health Organization classifications. Surgically resected tumor samples were immediately snap-frozen and subsequently stored in liquid nitrogen. For the mRNA expression assay, total RNAs were prepared from matched pairs of primary tumors and nearby normal lung tissues using TRIzol reagent (Invitrogen). cDNAs were synthesized using SuperScript RT (Invitrogen) according to the manufacturer's protocols. For IHC assay, surgically resected primary adenocarcinoma tissues were collected from 1995 to 1998 with approval by the Institutional Review Board of National Taiwan University Hospital (Taipei, Taiwan). Tissue sections (5 μm) were dewaxed and rehydrated. Antigen retrieval was done by incubating the slides in 0.01 M citric acid buffer at 100°C for 10 minutes. After blocking with 3% H_2O_2 and 5% FBS, the slides were reacted with a rabbit polyclonal Ab against hNaa10p diluted 1:300 at 4°C overnight. The slides were then incubated with polymer-HRP reagent (BioGenex). The peroxidase activity was visualized with diaminobenzidine tetrahydroxychloride (DAB) solution (BioGenix). The sections were counterstained with hematoxylin. Dark brown cytoplasmic staining was considered positive, and no staining was considered negative. For negative control, we replaced the primary Ab with 5% FBS. The proportion of tumor cells positive for hNaa10p varied considerably, ranging from diffuse positive (>50%), to focal (approximately 10%–50%), to trace (<10%).

Generation of stable clones by lentivirus infection, cell proliferation, soft agar, and NOD-SCID mouse tumorigenicity assays. Lentiviruses were generated according to the protocol of National RNAi Core Facility. H1299 cells were transduced with lentiviruses at MOI of approximately 3–10. After transduction, cells were selected by puromycin for 2 days. Selected cells were maintained in puromycin-containing medium. The knockdown efficiency was checked by Western blotting. For the cell proliferation assays shown in Figure 2C and Figure 4B, 2.5×10^4 cells/well were seeded in a 6-well plate the day before assay. At the indicated day, cells were trypsinized and counted by CASY TT (Innovatis). For soft agar assays, 2,000 cells were mixed with 0.37% complete RPMI–containing agar and seeded in the 6-well plate with 0.7% complete RPMI–containing agar for 2 weeks. Colonies were stained with 0.05% crystal violet, photographed, and counted by BioRad Quantity One software in triplicate. For NOD-SCID mouse tumorigenicity assays, 5×10^6 cells were subcutaneously injected into 8-week-old male NOD-SCID mice. The tumor size was measured on the indicated days, and tumor volume was calculated as $(l \times w^2)/2$, where l is length and w is width (both in millimeters).

IP, Western blot, and luciferase assay. IP was performed as described previously (68), except that cells were lysed in NP-40 buffer (50 mM Tris-HCl, 120 mM NaCl, and 0.5% NP-40) containing protease inhibitor mixture (Complete; Roche Molecular Biochemicals). Western blot and luciferase assays were performed as reported previously (69). For luciferase assays, the luciferase intensity was normalized to the corresponding protein concentration.

GST pulldown and EMSA. E. coli–expressed his-hNaa10p was purified by Ni-Sepharose 6 Fast Flow (Amersham Bioscience) according to the supplier's instructions (Qiagen) and further dialyzed against DNMT assay buffer (50 mM Tris, pH 8.0; 1.0 mM EDTA; 1.0 mM DTT; 10% glycerol; 1% Tween 80; 1 mM PMSF; and 1 mM DTT). Purification of GST-fused proteins for GST pulldown assays was carried out as reported previously (70), with minor modifications. The in vitro translated hNaa10p fragments (TNT system; Promega) pulled down by GST-DNMT1 fragments were subjected to Western blot analysis with corresponding Ab. EMSA assays were performed by mixing BSA or indicated proteins and 1 μl biotin-labeled hemimethylated DNA probes (Purigo Biotech) in 20 μl reaction buffer containing 5-fold Q buffer (20 mM HEPES, pH 7.9; 8% glycerol; 0.5 mM EDTA; 0.1 M KCl; 0.5 mM DTT; and 0.5 mM PMSF) and 0.1 μg poly dA-dT (P5782; Sigma-Aldrich). Reaction mixtures were separated by a 4% or 10% native acrylamide gel in 0.5× TBE containing 5% glycerol and further analyzed by Streptavidin-HRP (Jackson ImmunoResearch).

DNMT assay. Cells were collected and suspend in buffer A (10 mM HEPES, pH 8.0; 1.5 mM $MgCl_2$; 10 mM KCl; and 0.5% NP-40) containing protease inhibitor mixture (Complete; Roche Molecular Biochemicals). After centrifugation, the supernatant was removed, and the pellet was lysed in buffer C (20 mM HEPES, pH 8.0; 25% glycerol; 0.42 M NaCl; 1.5 mM $MgCl_2$; and 0.2 mM EDTA) containing protease inhibitor mixture (Complete; Roche Molecular Biochemicals), followed by dialysis against buffer D (20 mM HEPES, pH 8.0; 20% glycerol; 100 mM KCl; 0.2 mM EDTA; 0.5 mM PMSF; and 0.5 mM DTT). The DNMT assays shown in Figure 5, A and B, were performed as described previously (71), with some modifications. 20 μg nuclear lysate was mixed with 0.5 μg poly dI-dC (Sigma-Aldrich) and 3 μCi [methyl-^{3}H]-AdoMet (PerkinElmer) in 15 μl reaction buffer (50 mM Tris, pH 8.0; 1.0 mM EDTA; 1.0 mM DTT; 10% glycerol; and 1% Tween 80) at 37°C for 2 hours. Stop solution (1% SDS, 2 mM EDTA, 5% butanol, 0.25 mg/ml salmon sperm DNA, 125 mM NaCl, and 1 mg/ml proteinase K) was then added, and the mixture was further incubated at 37°C for another 30 minutes. DNAs were ethanol precipitated, resuspended in 0.3 N NaOH, and spotted onto GF/C filters (Whatman). The filters were washed with 5% trichloroacetic acid and then with 70% ethanol. The radioactivity remained on filters was analyzed using a Beckman liquid scintillation counter. All reactions were carried out in triplicate. The DNMT assays shown in Figure 5C and Supplemental Figure 7 were similar to those described above, except that *E. coli*–expressed and –purified His-Xpress-hNaa10p and recombinant DNMT1 (New England Biolabs) were mixed with DNA oligo containing random CG-rich sequences (Purigo Biotech) (72).

ChIP and cDNA analysis. ChIP assays were performed as described previously (69), with minor modifications. Rabbit anti-DNMT1 (GTX13537; GeneTex) or anti-hNaa10p (generated in our laboratory) was used to IP DNMT1- or hNaa10p-bound DNAs, which were then analyzed on a LightCycler 480 (Roche) with LightCycler 480 SYBR Green I Master (Roche) using DNA primers against E-cadherin (73) or p21 (74) promoter regions. The amounts of IP DNAs were quantified and calculated as follows: $[DNA_{IP}] - [DNA_{IgG}]/[DNA_{input}]$ (75). To measure the mRNA level, total RNAs were collected using TRIzol reagent (Invitrogen) and

converted into cDNA by SuperScript II RT (Invitrogen). Real-time PCR was performed using the LightCycler 480 (Roche) according to the manufacturer's instructions. All real-time PCR was done in triplicate.

Bisulfite sequencing. Cells were harvested in lysis buffer (50 mM Tris, pH 8.5; 1 mM EDTA; 0.5% Tween 20; and 2 mg/ml proteinase K). After overnight incubation at 55°C, DNAs were extracted by phenol/chloroform and precipitated by ethanol. Genomic DNA (1 μg) was bisulfite-converted by EZ DNA Methylation-Gold kit (Zymo Research Co.) according to the manufacturer's instructions. Converted genomic DNA (50 ng) was subjected to PCR with primers listed in Supplemental Table 1. Amplification was carried out as follows: 95°C for 30 seconds, 53°C for 30 seconds, and 72°C for 30 seconds, repeated for 35 cycles. The final PCR product was cloned into plasmid pCR II using a TA cloning kit (Invitrogen). Isolated plasmids were sequenced using ABI 3730 XL DNA Analyzer with T7 primer (service from Genomics BioSci & Tech Inc.).

Statistics. The survival probability was calculated by Kaplan-Meier method according to the hNaa10p IHC staining results. Statistical analysis was performed with SPSS. A P value less than 0.05 was considered significant.

Acknowledgments

We thank Y.M. Jeng (National Taiwan University Hospital, Taipei, Taiwan) for providing IHC staining and survival probability, Y.S. Chang (Chang-Gung University, Taoyuan, Taiwan), C.K.J. Shen (Academia Sinica, Taipei, Taiwan), and K.L. Jang (Pusan National University, Busan, South Korea) for providing plasmids; the National RNAi Core Facility, Taiwan (supported by the National Research Program for Genomic Medicine Grants of NSC), for shRNA vector; Y. Zhang, W.H. Lee, Y.M. Jeng, J.L. Workman, S. Galande, H.M. Shih, and M.C. Hung for valuable suggestions; Y. Zhang for critical editing of the manuscript; S.Y. Tung for published microarray database analysis; and P.H. Hsu for technical support. The study was primarily supported by grants from Academia Sinica, NRPGM/DOH, and MOEA to L.-J. Juan, and further supported in part by NHRI grants to L.-J. Juan and C.-W. Wu and NIH grant GM049245 to X. Cheng and A.K. Upadhyay.

Received for publication January 11, 2010, and accepted in revised form May 12, 2010.

Address correspondence to: Cheng-Wen Wu, Institute of Biomedical Sciences, Academia Sinica, 128 Academia Road, Section 2, Nankang, Taipei 115, Taiwan. Phone: 886.2.2652.3015; Fax: 886.2.2652.3075; E-mail: ken@ibms.sinica.edu.tw. Or to: Li-Jung Juan, Genomics Research Center, Academia Sinica, 128 Academia Road, Section 2, Nankang, Taipei 115, Taiwan. Phone: 886.2.2787.1234; Fax: 866.2.2789.8811; E-mail: ljjuan@gate.sinica.edu.tw.

1. Issa JP, et al. Increased cytosine DNA-methyltransferase activity during colon cancer progression. *J Natl Cancer Inst*. 1993;85(15):1235–1240.
2. Vertino PM, Issa JP, Pereira-Smith OM, Baylin SB. Stabilization of DNA methyltransferase levels and CpG island hypermethylation precede SV40-induced immortalization of human fibroblasts. *Cell Growth Differ*. 1994;5(12):1395–1402.
3. Belinsky SA, Nikula KJ, Baylin SB, Issa JP. A microassay for measuring cytosine DNA methyltransferase activity during tumor progression. *Toxicol Lett*. 1995;82–83:335–340.
4. Belinsky SA, Nikula KJ, Baylin SB, Issa JP. Increased cytosine DNA-methyltransferase activity is target-cell-specific and an early event in lung cancer. *Proc Natl Acad Sci U S A*. 1996;93(9):4045–4050.
5. Vertino PM, Yen RW, Gao J, Baylin SB. De novo methylation of CpG island sequences in human fibroblasts overexpressing DNA (cytosine-5-)-methyltransferase. *Mol Cell Biol*. 1996;16(8):4555–4565.
6. Ooi SK, O'Donnell AH, Bestor TH. Mammalian cytosine methylation at a glance. *J Cell Sci*. 2009;122(pt 16):2787–2791.
7. Gronbaek K, Hother C, Jones PA. Epigenetic changes in cancer. *Apmis*. 2007;115(10):1039–1059.
8. MacLeod AR, Rouleau J, Szyf M. Regulation of DNA methylation by the Ras signaling pathway. *J Biol Chem*. 1995;270(19):11327–11337.
9. McCabe MT, Low JA, Imperiale MJ, Day ML. Human polyomavirus BKV transcriptionally activates DNA methyltransferase 1 through the pRb/E2F pathway. *Oncogene*. 2006;25(19):2727–2735.
10. Torrisani J, Unterberger A, Tendulkar SR, Shikimi K, Szyf M. AUF1 cell cycle variations define genomic DNA methylation by regulation of DNMT1 mRNA stability. *Mol Cell Biol*. 2007;27(1):395–410.
11. Esteve PO, et al. Regulation of DNMT1 stability through SET7-mediated lysine methylation in mammalian cells. *Proc Natl Acad Sci U S A*. 2009;106(13):5076–5081.
12. Wang J, et al. The lysine demethylase LSD1 (KDM1) is required for maintenance of global DNA methylation. *Nat Genet*. 2009;41(1):125–129.
13. Esteve PO, et al. Direct interaction between DNMT1 and G9a coordinates DNA and histone methylation during replication. *Genes Dev*. 2006;20(22):3089–3103.
14. Vire E, et al. The Polycomb group protein EZH2 directly controls DNA methylation. *Nature*. 2006;439(7078):871–874.
15. Di Croce L, et al. Methyltransferase recruitment and DNA hypermethylation of target promoters by an oncogenic transcription factor. *Science*. 2002;295(5557):1079–1082.
16. Polevoda B, Arnesen T, Sherman F. A synopsis of eukaryotic Nalpha-terminal acetyltransferases: nomenclature, subunits and substrates. *BMC Proc*. 2009;(3 suppl 6):S2.
17. Polevoda B, Sherman F. N-terminal acetyltransferases and sequence requirements for N-terminal acetylation of eukaryotic proteins. *J Mol Biol*. 2003;325(4):595–622.
18. Arnesen T, et al. Proteomics analyses reveal the evolutionary conservation and divergence of N-terminal acetyltransferases from yeast and humans. *Proc Natl Acad Sci U S A*. 2009;106(20):8157–8162.
19. Whiteway M, Szostak JW. The ARD1 gene of yeast functions in the switch between the mitotic cell cycle and alternative developmental pathways. *Cell*. 1985;43(2 pt 1):483–492.
20. Hwang CS, Shemorry A, Varshavsky A. N-terminal acetylation of cellular proteins creates specific degradation signals. *Science*. 2010;327(5968):973–977.
21. Aparicio OM, Billington BL, Gottschling DE. Modifiers of position effect are shared between telomeric and silent mating-type loci in S. cerevisiae. *Cell*. 1991;66(6):1279–1287.
22. Whiteway M, Freedman R, Van Arsdell S, Szostak JW, Thorner J. The yeast ARD1 gene product is required for repression of cryptic mating-type information at the HML locus. *Mol Cell Biol*. 1987;7(10):3713–3722.
23. Jeong JW, et al. Regulation and destabilization of HIF-1alpha by ARD1-mediated acetylation. *Cell*. 2002;111(5):709–720.
24. Chang CC, et al. Effect of connective tissue growth factor on hypoxia-inducible factor 1alpha degradation and tumor angiogenesis. *J Natl Cancer Inst*. 2006;98(14):984–995.
25. Arnesen T, et al. Interaction between HIF-1 alpha (ODD) and hARD1 does not induce acetylation and destabilization of HIF-1 alpha. *FEBS Lett*. 2005;579(28):6428–6432.
26. Bilton R, et al. Arrest-defective-1 protein, an acetyltransferase, does not alter stability of hypoxia-inducible factor (HIF)-1alpha and is not induced by hypoxia or HIF. *J Biol Chem*. 2005;280(35):31132–31140.
27. Fisher TS, Etages SD, Hayes L, Crimin K, Li B. Analysis of ARD1 function in hypoxia response using retroviral RNA interference. *J Biol Chem*. 2005;280(18):17749–17757.
28. Shin DH, Chun YS, Lee KH, Shin HW, Park JW. Arrest defective-1 controls tumor cell behavior by acetylating myosin light chain kinase. *PLoS One*. 2009;4(10):e7451.
29. Kuo HP, et al. ARD1 stabilization of TSC2 suppresses tumorigenesis through the mTOR signaling pathway. *Sci Signal*. 2010;3(108):ra9.
30. Lim JH, Park JW, Chun YS. Human arrest defective 1 acetylates and activates beta-catenin, promoting lung cancer cell proliferation. *Cancer Res*. 2006;66(22):10677–10682.
31. Arnesen T, Gromyko D, Pendino F, Ryningen A, Varhaug JE, Lillehaug JR. Induction of apoptosis in human cells by RNAi-mediated knockdown of hARD1 and NATH, components of the protein N-alpha-acetyltransferase complex. *Oncogene*. 2006;25(31):4350–4360.
32. Gromyko D, Arnesen T, Ryningen A, Varhaug JE, Lillehaug JR. Depletion of the human N(alpha)-terminal acetyltransferase A (hNatA) induces p53-dependent apoptosis and p53-independent growth inhibition [published online ahead of print February 22, 2010]. *Int J Cancer*. doi: 10.1002/ijc.25275.
33. Yu M, et al. Immunohistochemical analysis of human arrest-defective-1 expressed in cancers in vivo. *Oncol Rep*. 2009;21(4):909–915.
34. Ren T, et al. Generation of novel monoclonal antibodies and their application for detecting ARD1 expression in colorectal cancer. *Cancer Lett*. 2008;264(1):83–92.
35. Midorikawa Y, et al. Identification of genes associated with dedifferentiation of hepatocellular carcinoma with expression profiling analysis. *Jpn J Cancer Res*. 2002;93(6):636–643.
36. Arnesen T, Thompson PR, Varhaug JE, Lillehaug JR. The protein acetyltransferase ARD1: a novel cancer drug target? *Curr Cancer Drug Targets*. 2008;8(7):545–553.
37. Kuo HP, Hung MC. Arrest-defective-1 protein

(ARD1): tumor suppressor or oncoprotein? *Am J Transl Res*. 2010;2(1):56–64.
38. Suzuki M, Sunaga N, Shames DS, Toyooka S, Gazdar AF, Minna JD. RNA interference-mediated knockdown of DNA methyltransferase 1 leads to promoter demethylation and gene re-expression in human lung and breast cancer cells. *Cancer Res*. 2004;64(9):3137–3143.
39. Asaumi M, et al. Interaction of N-terminal acetyltransferase with the cytoplasmic domain of beta-amyloid precursor protein and its effect on A beta secretion. *J Biochem*. 2005;137(2):147–155.
40. Jones PA, Baylin SB. The epigenomics of cancer. *Cell*. 2007;128(4):683–692.
41. Esteller M. Aberrant DNA methylation as a cancer-inducing mechanism. *Annu Rev Pharmacol Toxicol*. 2005;45:629–656.
42. Issa JP. CpG island methylator phenotype in cancer. *Nat Rev Cancer*. 2004;4(12):988–993.
43. Wang G, Hu X, Lu C, Su C, Luo S, Luo ZW. Promoter-hypermethylation associated defective expression of E-cadherin in primary non-small cell lung cancer. *Lung Cancer*. 2008;62(2):162–172.
44. Grady WM, et al. Methylation of the CDH1 promoter as the second genetic hit in hereditary diffuse gastric cancer. *Nat Genet*. 2000;26(1):16–17.
45. Bostick M, Kim JK, Esteve PO, Clark A, Pradhan S, Jacobsen SE. UHRF1 plays a role in maintaining DNA methylation in mammalian cells. *Science*. 2007;317(5845):1760–1764.
46. Sharif J, et al. The SRA protein Np95 mediates epigenetic inheritance by recruiting Dnmt1 to methylated DNA. *Nature*. 2007;450(7171):908–912.
47. Lee PJ, Washer LL, Law DJ, Boland CR, Horon IL, Feinberg AP. Limited up-regulation of DNA methyltransferase in human colon cancer reflecting increased cell proliferation. *Proc Natl Acad Sci U S A*. 1996;93(19):10366–10370.
48. Aoki E, Ohashi H, Uchida T, Murate T, Saito H, Kinoshita T. Expression levels of DNA methyltransferase genes do not correlate with p15INK4B gene methylation in myelodysplastic syndromes. *Leukemia*. 2003;17(9):1903–1904.
49. Eads CA, Danenberg KD, Kawakami K, Saltz LB, Danenberg PV, Laird PW. CpG island hypermethylation in human colorectal tumors is not associated with DNA methyltransferase overexpression. *Cancer Res*. 1999;59(10):2302–2306.
50. Kim H, et al. Elevated mRNA levels of DNA methyltransferase-1 as an independent prognostic factor in primary nonsmall cell lung cancer. *Cancer*. 2006;107(5):1042–1049.
51. Belinsky SA. Gene-promoter hypermethylation as a biomarker in lung cancer. *Nat Rev Cancer*. 2004;4(9):707–717.
52. Gottardi CJ, Wong E, Gumbiner BM. E-cadherin suppresses cellular transformation by inhibiting beta-catenin signaling in an adhesion-independent manner. *J Cell Biol*. 2001;153(5):1049–1060.
53. Stockinger A, Eger A, Wolf J, Beug H, Foisner R. E-cadherin regulates cell growth by modulating proliferation-dependent beta-catenin transcriptional activity. *J Cell Biol*. 2001;154(6):1185–1196.
54. Ke H, et al. Putative tumor suppressor Lats2 induces apoptosis through downregulation of Bcl-2 and Bcl-x(L). *Exp Cell Res*. 2004;298(2):329–338.
55. Cho WJ, et al. miR-372 regulates cell cycle and apoptosis of ags human gastric cancer cell line through direct regulation of LATS2. *Mol Cells*. 2009;28(6):521–527.
56. Wang F, et al. Transcriptional repression of WEE1 by Kruppel-like factor 2 is involved in DNA damage-induced apoptosis. *Oncogene*. 2005; 24(24):3875–3885.
57. Su LJ, et al. Selection of DDX5 as a novel internal control for Q-RT-PCR from microarray data using a block bootstrap re-sampling scheme. *BMC Genomics*. 2007;8:140.
58. Landi MT, et al. Gene expression signature of cigarette smoking and its role in lung adenocarcinoma development and survival. *PLoS One*. 2008; 3(2):e1651.
59. Spira A, et al. Airway epithelial gene expression in the diagnostic evaluation of smokers with suspect lung cancer. *Nat Med*. 2007;13(3):361–366.
60. Strazisar M, Mlakar V, Glavac D. LATS2 tumour specific mutations and down-regulation of the gene in non-small cell carcinoma. *Lung Cancer*. 2009;64(3):257–262.
61. Aylon Y, et al. Silencing of the Lats2 tumor suppressor overrides a p53-dependent oncogenic stress checkpoint and enables mutant H-Ras-driven cell transformation. *Oncogene*. 2009;28(50):4469–4479.
62. Takahashi Y, et al. Down-regulation of LATS1 and LATS2 mRNA expression by promoter hypermethylation and its association with biologically aggressive phenotype in human breast cancers. *Clin Cancer Res*. 2005;11(4):1380–1385.
63. Jiang Z, et al. Promoter hypermethylation-mediated down-regulation of LATS1 and LATS2 in human astrocytoma. *Neurosci Res*. 2006;56(4):450–458.
64. Varambally S, et al. Integrative genomic and proteomic analysis of prostate cancer reveals signatures of metastatic progression. *Cancer Cell*. 2005;8(5):393–406.
65. Hong Y, Ho KS, Eu KW, Cheah PY. A susceptibility gene set for early onset colorectal cancer that integrates diverse signaling pathways: implication for tumorigenesis. *Clin Cancer Res*. 2007;13(4):1107–1114.
66. Dyrskjot L, et al. Gene expression in the urinary bladder: a common carcinoma in situ gene expression signature exists disregarding histopathological classification. *Cancer Res*. 2004;64(11):4040–4048.
67. Hippo Y, et al. Global gene expression analysis of gastric cancer by oligonucleotide microarrays. *Cancer Res*. 2002;62(1):233–240.
68. Hsu CH, et al. HCMV IE2-mediated inhibition of HAT activity downregulates p53 function. *EMBO J*. 2004;23(11):2269–2280.
69. Lee SB, Ou DS, Lee CF, Juan LJ. Gene-specific Transcriptional Activation Mediated by the p150 Subunit of the Chromatin Assembly Factor 1. *J Biol Chem*. 2009;284(21):14040–14049.
70. Juan LJ, et al. Histone deacetylases specifically down-regulate p53-dependent gene activation. *J Biol Chem*. 2000;275(27):20436–20443.
71. Tsai CN, Tsai CL, Tse KP, Chang HY, Chang YS. The Epstein-Barr virus oncogene product, latent membrane protein 1, induces the downregulation of E-cadherin gene expression via activation of DNA methyltransferases. *Proc Natl Acad Sci U S A*. 2002;99(15):10084–10089.
72. Yokochi T, Robertson KD. Preferential methylation of unmethylated DNA by Mammalian de novo DNA methyltransferase Dnmt3a. *J Biol Chem*. 2002;277(14):11735–11745.
73. Jung JK, Arora P, Pagano JS, Jang KL. Expression of DNA methyltransferase 1 is activated by hepatitis B virus X protein via a regulatory circuit involving the p16INK4a-cyclin D1-CDK 4/6-pRb-E2F1 pathway. *Cancer Res*. 2007;67(12):5771–5778.
74. McKinney K, Mattia M, Gottifredi V, Prives C. p53 linear diffusion along DNA requires its C terminus. *Mol Cell*. 2004;16(3):413–424.
75. Makar KW, Perez-Melgosa M, Shnyreva M, Weaver WM, Fitzpatrick DR, Wilson CB. Active recruitment of DNA methyltransferases regulates interleukin 4 in thymocytes and T cells. *Nat Immunol*. 2003;4(12):1183–1190.